Parallel domain decomposition preconditioners for Isogeometric discretizations arising in impact problems at high strain rates

Luc Berger-Vergiat[a,*]

[a]*Department of Civil Engineering & Engineering Mechanics, Columbia University, New York, NY 10027*

Abstract

Shear bands are micron size narrow bands of intense plastic deformations that form in metals subjected high strain rates such as in impact or blast. Their formation is associated with significant heating and they are also considered material instabilities which precede fracture. The aim of this work is to develop fast converging Isogeometric elements for monolithic solution of shear bands and appropriate parallel and iterative solvers that are robust through all the deformation stages: homogeneous, onset of instability and stress collapse. To this end, we propose irreducible and hybrid NURBS quadrilateral elements that are stable and locking free and lead to high rates of convergence. To solve the resulting linearized systems, a novel Schur based domain-decomposition preconditioners are proposed based on constitutive/conservation laws splitting. The elements and solvers are implemented in parallel and shows excellent scaling performance compared to standard solvers.

Keywords: Shear bands, NURBS, Preconditioner, Schur complement, Domain decomposition, Additive Schwarz method

1. Introduction: Governing equations of shear bands

Recent work on shear band [8, 2] reformulated the numerical model as a mixed formulation of coupled thermo-mechanical set of equations with diffusive regularization. Diffusion serves to introduce an implicit length scale, governed by competition between shear heating and conduction, and will regularize the problem in the softening regime. The problem is thus modeled using the following system of four coupled equations

$$\begin{cases} \rho\ddot{\underline{u}} - \underline{\nabla} \cdot \underline{\underline{\sigma}} - \underline{f}^{ext} = 0 \\ \dot{T} - \kappa\Delta T - \chi\bar{\sigma}\dot{\bar{\gamma}}_p = 0 \\ \underline{\underline{\dot{\sigma}}} - \underline{\underline{\underline{\underline{C}}}}^{elas} : \left(\underline{\underline{\dot{\varepsilon}}} - \underline{\underline{\dot{\varepsilon}}}^{p} - \underline{\underline{\dot{\varepsilon}}}^{T}\right) = 0 \\ \dot{\bar{\gamma}}_p - g(\bar{\sigma}, T, \bar{\gamma}_p) = 0 \end{cases} \tag{1}$$

*Corresponding author

Email address: luc.berger@columbia.edu (Luc Berger-Vergiat)

where $\underline{u}$, T, $\underline{\underline{\sigma}}$ and $\bar{\gamma}_p$ are the displacement, temperature, stress and equivalent plastic strain variables respectively. These fields are underlined according to their tensorial order ($\underline{u}$ is a first order tensor and the strain $\underline{\underline{\varepsilon}} = \underline{\nabla}^s \underline{u}$ is a second order tensor), $\bar{\sigma}$ is the equivalent stress defined as $\bar{\sigma} = \sqrt{\frac{3}{2}\underline{\underline{S}} : \underline{\underline{S}}}$ with $\underline{\underline{S}} = \underline{\underline{\sigma}} - \frac{\underline{\underline{I}}:\underline{\underline{\sigma}}}{3}\underline{\underline{I}}$, κ and χ are the thermal conductivity and the Taylor-Quinney coefficient, finally $\underline{\nabla} \cdot \bullet$ and $\underline{\nabla}^s \bullet$ denotes the divergence and symmetric gradient operators.
Time integration is performed using the Newmark-β algorithm ($\beta = \frac{1}{4},\ \gamma = \frac{1}{2}$), the nonlinear problem is solved with a Newton algorithm and Eq. 1 is linearized using a first order approximation of the residual with a Gâteaux derivative

$$\mathbf{R}(\underline{u} + \epsilon\delta\underline{u}) \approx \mathbf{R}(\underline{u}) + \frac{d\mathbf{R}}{d\epsilon}(\underline{u} + \epsilon\delta\underline{u})\bigg|_{\epsilon=0}, \tag{2}$$

for instance $\mathbf{J}_{u\sigma}\delta\underline{\underline{\sigma}}$ is computed as follows

$$\begin{aligned}
\mathbf{J}_{u\sigma}\delta\underline{\underline{\sigma}} &= \frac{d\mathbf{R}_u(\underline{\underline{\sigma}} + \epsilon\delta\underline{\underline{\sigma}})}{d\epsilon}\bigg|_{\epsilon=0} \\
&= \frac{d}{d\epsilon}\left(\int_\Omega w_u \rho \frac{\partial^2 \underline{u}}{\partial t^2} + \underline{\nabla}\ w_u \cdot (\underline{\underline{\sigma}} + \epsilon\delta\underline{\underline{\sigma}})d\Omega - \int_{\Gamma_t} w_u \underline{\bar{t}} d\Gamma_t\right)\bigg|_{\epsilon=0} \\
&= \int_\Omega \underline{\nabla}\ w_u \cdot \delta\underline{\underline{\sigma}} d\Omega,
\end{aligned} \tag{3}$$

finally the spacial discretization is obtained using the finite element method. This procedure results in a succession of linear algebra problems that we solve at each Newton iteration

$$\left[\begin{array}{cc:cc}
\mathbf{J}_{\underline{u}\underline{u}} & \mathbf{J}_{\underline{u}T} & \mathbf{J}_{\underline{u}\underline{\underline{\sigma}}} & \mathbf{J}_{\underline{u}\bar{\gamma}_p} \\
\mathbf{J}_{T\underline{u}} & \mathbf{J}_{TT} & \mathbf{J}_{T\underline{\underline{\sigma}}} & \mathbf{J}_{T\bar{\gamma}_p} \\
\hdashline
\mathbf{J}_{\underline{\underline{\sigma}}\underline{u}} & \mathbf{J}_{\underline{\underline{\sigma}}T} & \mathbf{J}_{\underline{\underline{\sigma}}\underline{\underline{\sigma}}} & \mathbf{J}_{\underline{\underline{\sigma}}\bar{\gamma}_p} \\
\mathbf{J}_{\bar{\gamma}_p\underline{u}} & \mathbf{J}_{\bar{\gamma}_pT} & \mathbf{J}_{\bar{\gamma}_p\underline{\underline{\sigma}}} & \mathbf{J}_{\bar{\gamma}_p\bar{\gamma}_p}
\end{array}\right]
\left[\begin{array}{c}
\delta\underline{u} \\ \delta T \\ \hdashline \delta\underline{\underline{\sigma}} \\ \delta\bar{\gamma}_p
\end{array}\right] =
\left[\begin{array}{c}
\mathbf{R}_{\underline{u}} \\ \mathbf{R}_T \\ \hdashline \mathbf{R}_{\underline{\underline{\sigma}}} \\ \mathbf{R}_{\bar{\gamma}_p}
\end{array}\right]
\Leftrightarrow
\left[\begin{array}{c:c}
\mathbf{J}_{\alpha\alpha} & \mathbf{J}_{\alpha\eta} \\ \hdashline \mathbf{J}_{\eta\alpha} & \mathbf{J}_{\eta\eta}
\end{array}\right]
\left[\begin{array}{c}
\delta\alpha \\ \hdashline \delta\eta
\end{array}\right] =
\left[\begin{array}{c}
\mathbf{R}\alpha \\ \hdashline \mathbf{R}\eta
\end{array}\right] \tag{4}$$

This Jacobian matrix is non-symmetric due to the thermo-mechanical couplings and to the nonlinearities introduced by the plasticity. The plastic nonlinearities affect the problem differently depending on the stage of the shear band: onset of plasticity, thermal softening and stress collapse see Fig. 1, this leads to varying properties for the Jacobian such as varying coupling strength and varying condition number with strong degradation of the spectral radius during the stress collapse phase that can lead to ill-conditioned linear systems. However with this approach the shear band localization is naturally regularized and it has been shown to lead to mesh insensitive simulations.

2. Isogeometric discretization of shear bands

The choice of shape functions in the discretization of Eq. 4 is critical to achieve stability and fast convergence of the simulation. Previous work [8] utilized the Pian and Sumihara

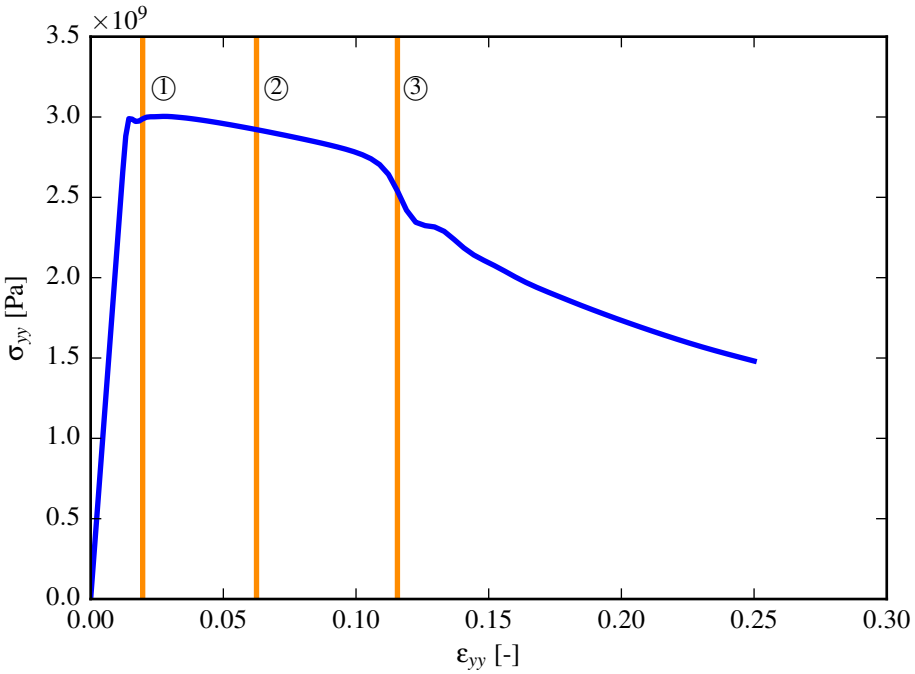

Figure 1: Typical stress-strain curve for the formation of a shear band with the beginning of the three stages marked as: ① onset of plasticity, ② thermal softening, ③ stress collapse.

shape functions associated with linear shape functions for the displacement and temperature and Gauss points variables for the equivalent plastic strain. The use Pian and Sumihara shape functions reduced considerably the amount of volumetric locking during the shear band formation due to the $J2$ plastic flow law.

Here to retain this property and increase the convergence rate of the formulation, displacement and temperatures are discretized using isogeometric concepts [2]. In this framework it is not possible to use Pian and Sumihara's approach anymore so we rely on the $\overline{\mathrm{B}}$-bar technique associated to the higher order NURBS shape functions to overcome volumetric locking. Functions continuous across elements are not suited for the discretization of the equivalent plastic strain since it leads to oscillations and non-physical behaviors of the material. Finally the stress has been shown to be stable even when discretized with NURBS shape functions of lower order than the displacement which is somewhat counter intuitive. Mesh insensitive simulation with low level of volumetric locking are achieved with the proposed elements as presented in Fig. 2

The convergence of the HNSQ convergence with different shape functions order is compared to the Pian and Sumihara on a plate under uniaxial tension with a central imperfection. We can see from Table 1 that the HNSQ element proves to be more accurate and to converge faster than the PSSQ element.

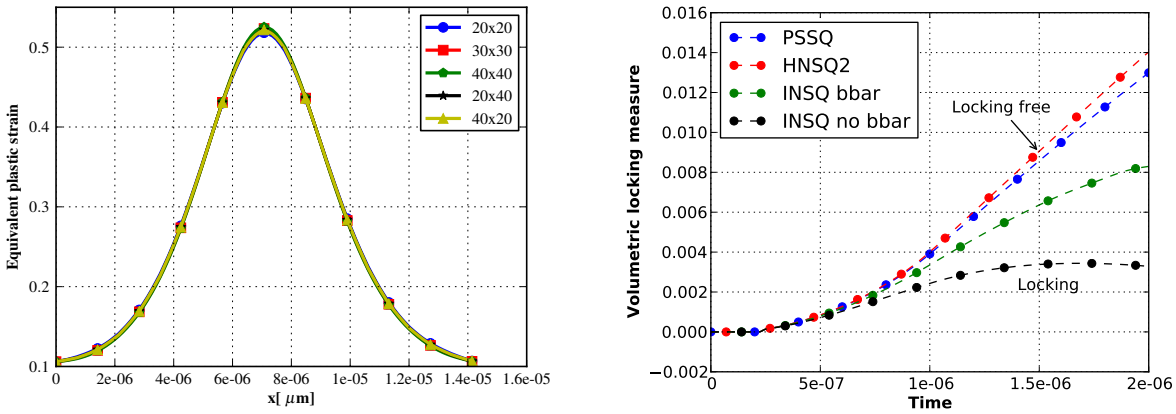

Figure 2: Left: mesh insensitive results using INSQ element. Right: comparison of volumetric locking for Pian and Sumihara (PSSQ), hybrid NURBS (HNSQ2) and Irreducible NURBS (INSQ) shear band quadrilateral elements.

	PS	P1	P2	P3	P4
10×10	3.4835e-03	1.8633e-03	1.8442e-04	2.7998e-04	5.9015e-05
20×20	8.7363e-04	6.1263e-05	3.3638e-06	6.5635e-07	2.1772e-07
30×30	3.9042e-04	1.7651e-05	1.0837e-06	2.1221e-07	6.6989e-08
40×40	2.2004e-04	2.4556e-06	2.2975e-07	1.0033e-07	0.0000e+00

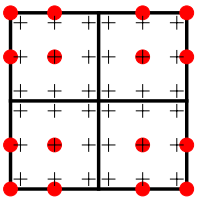

Table 1: Left: k-refinement and h-refinement comparison for HNSQ and PSSQ elements. Right: patch of four INSQ elements, red dots (•) indicate control points for displacement and temperature, black crosses (+) indicate nodes for stress and equivalent plastic strain.

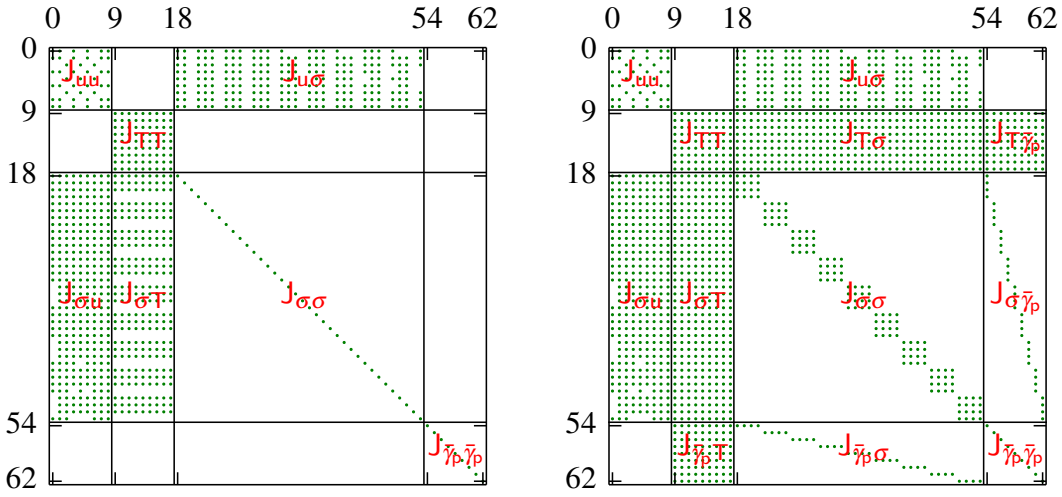

Figure 3: Sparsity pattern of a single Jacobian quadratic INSQ element matrix in the linear elastic (left) and nonlinear plastic (right) regime. The green dots (•) indicate nonzero terms and the black lines show the limits of the blocks in the matrix.

3. Parallel preconditioner for shear bands

The cost of inverting the linearized system Eq. 4 becomes quickly prohibitive as mesh resolution increases due to the large amount of degrees of freedom per nodes (8 dofs/node in 2D and 11 dofs/node in 3D). To reduce the cost and improve the scaling associated to inverting $\mathbf{J}$ we propose to use a Schur complement $\mathbf{S}$ that follows the conservation/constitutive laws split introduced with the α/η notation of Eq. 4 to construct a preconditioner for a gmres solver applied to $\mathbf{J}$. Forming $\mathbf{S} = \mathbf{J}_{\alpha\alpha} - \mathbf{J}_{\alpha\eta}\mathbf{J}_{\eta\eta}^{-1}\mathbf{J}_{\eta\alpha}$ can be expensive depending on the element chosen (expensive for HNSQ, cheap for INSQ) so we use an approximation $\mathbf{S}^* = \mathbf{J}_{\alpha\alpha} - \mathbf{J}_{\alpha\eta}\left[\mathrm{diag}\left(\mathbf{J}_{\eta\eta}\right)\right]^{-1}\mathbf{J}_{\eta\alpha}$. Finally $\mathbf{S}^*$ is inexactly inverted using either of two approximations:

1. a second Schur complement leading to a preconditioner denoted $\mathbf{P}_{Sr}$ and called Schur-Schur

$$(\mathbf{S}^*)^{-1} \approx \begin{bmatrix} \mathbf{1} & -(\mathbf{S}^*_{uu})^{-1}\mathbf{S}^*_{uT} \\ \mathbf{0} & \mathbf{1} \end{bmatrix} \begin{bmatrix} (\mathbf{S}^*_{uu})^{-1} & \mathbf{0} \\ \mathbf{0} & \mathbf{S}^{-1}_{inner} \end{bmatrix} \begin{bmatrix} \mathbf{1} & \mathbf{0} \\ -\mathbf{S}^*_{Tu}(\mathbf{S}^*_{uu})^{-1} & \mathbf{1} \end{bmatrix} \tag{5}$$

   with $\mathbf{S}_{inner} = \mathbf{S}^*_{TT} - \mathbf{S}^*_{Tu}\left[\mathrm{diag}(\mathbf{S}^*_{uu})\right]^{-1}\mathbf{S}^*_{uT}$, or
2. a non-overlapping multiplicative Schwarz preconditioner denoted $\mathbf{P}_{Sz}$ and called Schur-Schwarz

$$(\mathbf{S}^*)^{-1} \approx \mathbf{B}_0 + \mathbf{B}_1\mathbf{B}_1\mathbf{S}\mathbf{B}_0 \quad \text{with } \mathbf{B}_0 = \begin{bmatrix} (\mathbf{S}^*_{uu})^{-1} & \mathbf{0} \\ \mathbf{0} & \mathbf{1} \end{bmatrix} \text{ and } \mathbf{B}_1 = \begin{bmatrix} \mathbf{1} & \mathbf{0} \\ \mathbf{0} & (\mathbf{S}^*_{TT})^{-1} \end{bmatrix} \tag{6}$$

Weak and strong scaling of the proposed preconditioners are presented and compared to the scaling of an LU solver in Fig. 4. As we can see the proposed preconditioners exhibit

superior scaling properties compared to the LU solver making them useful alternatives for large system of equations. This is especially true for the Schur-Schwarz solver. Weak scaling tests reveal that both preconditioners also have better weak scaling than the LU solver and that the Schur-Schur preconditioner exhibit the best weak scaling capabilities see [3].

However as we will see in the next section, more optimized preconditioners can be obtained

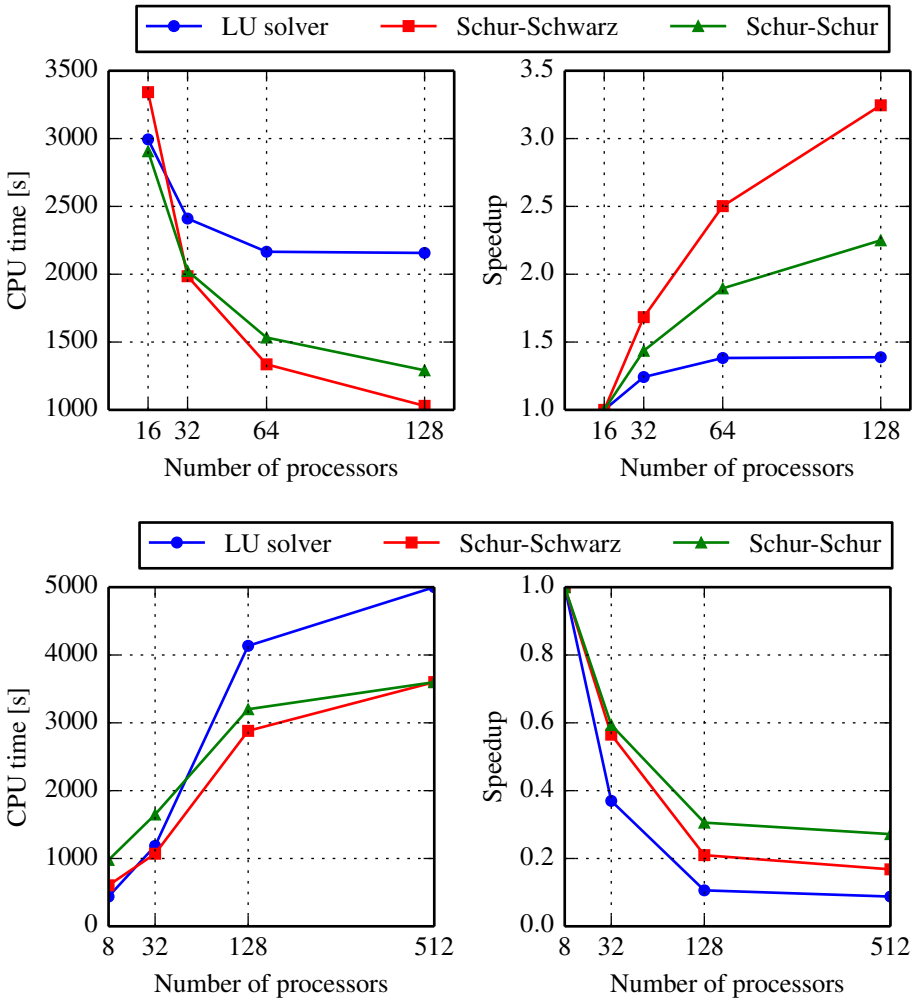

Figure 4: Top: Strong scaling of preconditioners $\mathbf{P}_{Sr}$ and $\mathbf{P}_{Sz}$ compared to an LU solver on a 320,000 equations system. Bottom: Weak scaling of the preconditioners compared to an LU solver 8000 equations per node.

if elements with discontinuous shape functions for stress and equivalent plastic strain field (such as INSQ or PSSQ) are used to discretize Eq. 4.

4. Modified domain decomposition predonditioner

Using the conservation/constitutive laws split presented in Eq. 4 as well as discontinuous shape functions (Pian and Sumihara or irreducible) for $\underline{\underline{\sigma}}$ and $\bar{\gamma}_p$ a Schur complement can be

used to efficiently eliminate the η variables and the linear solves required during the Newton iterations are re-cast as

$$\begin{cases} \mathbf{S}\delta\alpha = \mathbf{R}_\alpha - \mathbf{J}_{\alpha\eta}\mathbf{J}_{\eta\eta}^{-1}\mathbf{R}_\eta \\ \delta\eta = \mathbf{J}_{\eta\eta}^{-1}\left(\mathbf{R}_\eta - \mathbf{J}_{\eta\alpha}\delta\alpha\right) \end{cases} \tag{7}$$

with $\mathbf{S} = \mathbf{J}_{\alpha\alpha} - \mathbf{J}_{\alpha\eta}\mathbf{J}_{\eta\eta}^{-1}\mathbf{J}_{\eta\alpha}$. In this form the computational effort is greatly reduced compared to the cost associated with solving for the monolithic Jacobian. The computational effort is now concentrated in solving for the Schur complement matrix denoted $\mathbf{S}$.

In our approach $\mathbf{S}$ is approximately solved for using a preconditioned generalized minimal residual (gmres) iterative solver. To reduce further the cost of the simulation the localized nature of shear bands is leveraged using a domain decomposition approach [4]. The zone where the shear bands develops is is assigned to a subdomain denoted Ω_{sb} and called shear band subdomain, the zone not affected by the shear band is denote Ω_h and is called the healthy zone see Fig. 5. The domain decomposition technique used is a modified additive Schwarz method (ASM) such that at each Newton iterations the matrix associated to the healthy subdomain is kept identical to the initial matrix associated to that subdomain. Hence the inverse of the preconditioner $\mathbf{P}_{ASM_0}$ is expressed as

$$\mathbf{P}_{ASM_0}^{-1} = \left(\mathbf{S}_h^{lin}\right)^{-1} + \mathbf{S}_{sb}^{-1} \tag{8}$$

where $\mathbf{S}_h^{lin}$ and $\mathbf{S}_{sb}$ are defined according to the method proposed by Cai *et al.* [5]

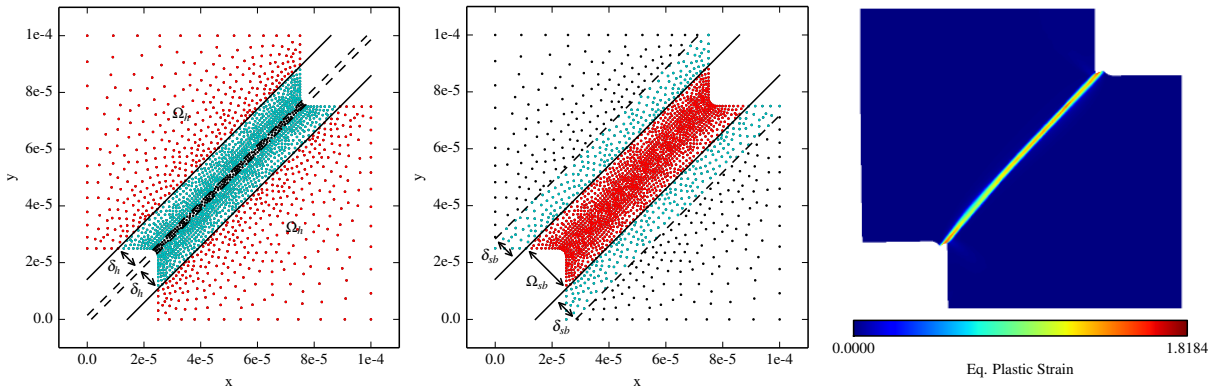

Figure 5: Representation of the healthy (left) and shear band (middle) subdomain containing the red nodes • and their overlap sets containing the blue nodes •. Equivalent plastic strain field (right) at the end of the simulation.

With this definition the cost required to invert the preconditioner is low because $\mathbf{S}_h^{lin}$ is inverted only once and then reused throughout the simulation. This is highly advantageous since Ω_h is typically large compared to Ω_{sb}. However if too much plastic strain develops in Ω_h the approximation $\mathbf{S}_h \approx \mathbf{S}_h^{lin}$ will lead to a slow convergence of the gmres solver.
In summary the algorithm used to invert the linearized systems at each Newton iterations

is written as

$$\begin{cases} \text{gmres}(\mathbf{S}, \mathbf{R}_\alpha - \mathbf{J}_{\alpha\eta}\mathbf{J}_{\eta\eta}^{-1}\mathbf{R}_\eta, \mathbf{P}_{ASM_0}^{-1}) \rightarrow \mathbf{x}_\alpha \\ \mathbf{J}_{\eta\eta}^{-1}\left(\mathbf{R}_\eta - \mathbf{J}_{\eta\alpha}\mathbf{x}_\alpha\right) \rightarrow \mathbf{x}_\eta \end{cases} . \tag{9}$$

The preconditioner is tested on the benchmark example shown in Fig. 5 with three different mesh resolution: coarse, medium and fine. It is compared to other solvers and preconditioners: an LU solver applied to the monolithic Jacobian $LU(\mathbf{J})$, an LU solver applied to the Schur complement matrix $LU(\mathbf{S})$, a gmres preconditioned by an ILU(0) algorithm applied to the Schur complement matrix gmres($\mathbf{S}$, ILU(0)) and finally ASM which is similar to ASM_0 without the approximation $\mathbf{S}_h \approx \mathbf{S}_h^{lin}$ hence in ASM the matrix associated with the healthy subdomain is updated and has to be inverted at each Newton iteration. The results associated this benchmark example are presented in Table 2.

Mesh	LU($\mathbf{J}$)	LU($\mathbf{S}$)	GMRES($\mathbf{S}$,ILU(0))	ASM	ASM_0
Coarse	373.36	401.91	399.93	401.31	332.81
Medium	1272.19	1260.48	1256.41	1242.89	1034.71
Fine	2909.45	2715.76	5015.37	1947.29	1828.12

Table 2: CPU times [s] for the simulation of the shear band under compression problem for three different meshes

On all the meshes the proposed preconditioner is performing best in terms of simulation time. Its performance is closely followed by that of the ASM preconditioner which provides almost as good a strong scaling as the ASM_0 preconditioner does.
The ILU(0) preconditioner performs very well on the coarsest mesh but its scaling is very poor. Furthermore, as expected the $LU(\mathbf{J})$ and $LU(\mathbf{S})$ preconditioners have the worst scaling, $LU(\mathbf{J})$ performing slightly better than $LU(\mathbf{S})$ on the coarsest mesh because of the time associated with the computation of the Schur complement, but forming the Schur complement proves to be a good option as the mesh is refined.

Finally the preconditioner is tested on a second benchmark: a square plate under uniaxial tension with an imperfection at its center, but for increasing polynomial order of NURBS shape functions. The preconditioner is compared to other state-of-the-practice solvers and results are presented in Table 3.
We observe that for low polynomial order the proposed preconditioners are not too advantageous but as the polynomial order is increased the performance of the proposed preconditioner improves compared to the other solution schemes. As it is the case for the first benchmark, the proposed preconditioner performs better on larger meshes even for low order elements see [4].

Conclusion

This work develops high order NURBS elements and iterative solvers for a difficult thermo-mechanics problem associated with the formation and propagation of shear bands.

Order	LU($\mathbf{J}$)	LU($\mathbf{S}$)	GMRES($\mathbf{S}$,ILU(0))	ASM	ASM_0
P1	31.71	30.58	30.51	32.82	33.62
P2	105.40	89.07	84.48	92.92	88.97
P3	315.05	254.55	251.24	253.56	252.48
P4	799.05	638.55	646.20	652.25	626.40

Table 3: CPU times [s] for the simulation of the shear band under compression problem for four different polynomial orders on a 20 by 20 elements mesh

These elements are shown to yield high convergence rates, alleviate volumetric locking and provide mesh independent results thanks to the implicit length scale introduced by the thermal diffusion. Specialized domain-decomposition preconditioners that take into account the physics and the specific discretization are developed and implemented for parallel computing and show excellent performance.
Future work will extend the solvers to the full brittle-ductile dynamic fracture model and account for adaptive and simultaneous propagation of shear bands and brittle cracks.

[1] L. Berger-Vergiat, H. Waisman, B. Hiriyur, R. Tuminaro, D. Keyes, *Inexact Schwarz-AMG preconditioners for crack problems modeled by XFEM*, Int. J. for Numer. Meth. in Engng., 90 (3) (2012) 311–328

[2] L. Berger-Vergiat, C. McAuliffe, H. Waisman, *Isogeometric analysis of shear bands*, Comp. Mech. 54 (2) (2014) 503–521.

[3] L. Berger-Vergiat, C. McAuliffe, H. Waisman, *Parallel preconditioners for monolithic solution of shear bands*, J. of Comp. Phys. 304 (2016) 359–379.

[4] L. Berger-Vergiat, H. Waisman, *A domain decomposition solution method for shear bands formation at high strain rates*, in preparation.

[5] X.-C. Cai, M. Sarkis, *A restricted additive Schwarz preconditioner for general sparse linear systems*, SIAM J. on Sci. Comp. 21 (2) (1999) 792–797.

[6] H. Elman, V.E. Howle, J.N. Shadid, R.R. Shuttleworth, R.S. Tuminaro, *A Taxonomy and Comparison of Parallel Block Multi-Level Preconditioners for the Incompressible Navier-Stokes Equations*, J. of Comp. Phys., 227 (3) (2008) 1790–1808.

[7] B. Hiriyur, R. Tuminaro, H. Waisman, E. Boman, D. Keyes, *A quasi-algebraic multigrid approach to fracture problems based on extended finite elements*, SIAM J. of Sci. Comp., 34 (2) (2012) A603–A626.

[8] C. McAuliffe, H. Waisman, *Mesh insensitive formulation for initiation and growth of shear bands using mixed finite elements*, Comp. Mech. 51 (5) (2013) 807–823.